Feasibility study of a CRS4 alternative spallation target for FASTEF

V. Moreau,

CRS4, Centre for Advanced Studies, Research and Development in Sardinia

July 16th 2010
Version 1.4 (Final)

Abstract

This document gathers some information on the free surface simulations with starccmV4.06 of preliminary versions of a CRS4 spallation target outsider candidate for the XT-ADS or FASTEF spallation target. The initial attempts are shortly illustrated and motivations for the changes are given. Once reasonably satisfied with the geometry, we test a rather simple condensation/sharpening algorithm on rather stiff operating conditions. Several variants, always based on a source/sink term for the light phase, are tested, systematically showing a degradation of the algorithm performances from the original algorithm. Finally, a full 3D loop of a potential candidate as spallation target with a sharp highly transient free-surface and a simplified thermal coupling is described and commented.

Contents

1 Introduction

In the framework of the FP6 EUROTRANS[1] **[3**] IP, a Myrrha-like Target has been foreseen for the XT-ADS[2] which in turn served as basis for the FP7 CDT[3]**[4**] project aiming at the construction of a Fast spectrum Transmutation Facility (FASTEF). This target must dissipate about 1.1MW from a 2.5 mA, 600MeV spallation beam (with a 72% thermal efficiency) within a very short space. It presents several difficult features from the CFD point of view. Mainly, it is a two-fluid flow composed of liquid Lead Bismuth Eutectic (LBE) and an extremely rarefied gas which can be considered as an almost perfect vacuum.

Our participation in the FP7 THINS[4] **[5**] project consists in trying to operate free-surface simulations an improve their range of application in the nuclear context both gaining know-how on existing models and also improving these models or creating new (better) ones. Therefore, studying

[1] EUROTRANS: EUROpean research programme for the TRANSmutation of high level nuclear waste in an accelerator driven system
[2] XT-ADS: eXperimenTal Accelerator Driven System
[3] CDT: Central Design Team
[4] Thermal Hydraulics of Innovative Nuclear Systems

the feasibility of an alternative windowless spallation target is perfectly in line with our THINS objectives.

The reference XT-ADS design consider a fundamentally axial-symmetrical free fall spallation target, with a small central recirculation zone. In the design, because of material issues, local velocities should remain below 2.5 m/s, the nominal flow rate being 13 l/s for a mean temperature increase about 50K. In the alternative design discussed here, we want to avoid the numerical difficulties associated with the axial-symmetrical central recirculation treatment. Moreover, in a former 2D+ simulation of a falling jet **[6**], it has not be possible to get a reasonably stable reattachment point where the free falling liquid should connect to the bulk fluid region. The reattachment instability is not clearly understood but may be related to the very small space available, the reattachment occurring in a quite small down coming pipe. The point is that we want to propose a design that we are able to confidently simulate numerically.

In the PDS-XADS FP5 project [2], a channel like target has already been dimensioned and simulated **[7**]. The simulations were very promising. However, they were made without considering directly an eventual deformation of the free surface. It should also be noted that the room available in the XT-ADS context is much less than in the PDS-XADS one. As the former 2D+ simulation have demonstrated the effective capacity to perform articulated and meaningful free-surface flow simulations, we investigate in this document the possibility to adapt the knowledge gained in PDS-XADS and the new free surface capability in the context of the XT-ADS or FASTEF.

2 Rounded diffuser option

The free surface simulations are performed with starccm+ versions 4.06. From the version 4.06 of starccm+, stardesign is strongly linked to starccm+ and the transfer to starccm+ can be effectuated as soon as the geometry is built in stardesign. Otherwise précised, default setting are used.

This series of test cases has been thought with the objective of having a relatively stable free surface subject to a relatively strong shear, associated to the free-surface numerical smearing. Dimensions and operating conditions should be reasonably in line with the foreseen XT-ADS and FASTEF spallation targets.

The first geometry, illustrated in Figure 1, is therefore enclosed in the external envelop of three vertical hexagonal tubes (the lobes) about XT-ADS size (diameter 10.5 cm) to obtain some result at some significant flow rate. The driving idea was to test a channel-like target, even if the geometry does not seems a priory very well suited. In fact, a channel-like target means 3D calculations from scratch (half-domain) with small time steps. That is a foreseeable failure after a long and painful “bath of blood”. By the way, hope was to get at least some clue for one of the main long term objective (an operable free-surface target). It should also be stressed that related (but without resolved free surface) 2D and 3D simulations had been already performed in the PDS-XADS framework.

Here is the basic idea. The flow rises from one lobe and is distributed to the central spallation region by a differentiated flow filtering grid. The grid is differentiated so has to be less resistive towards the top, therefore promoting a nearly horizontal flow faster near the free surface than in the bulk, still delivering there a consistent flow. After flowing horizontally in the central region, the flow is separated to fall down into the two other lobes.

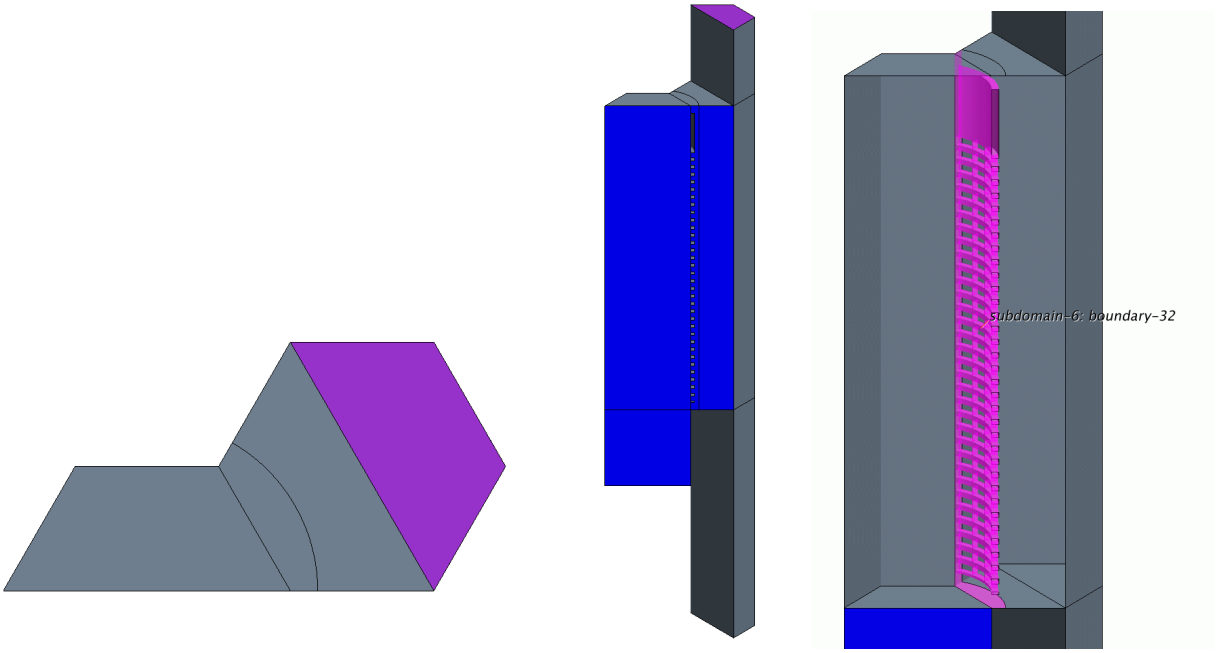

Figure 1: CRS4 target. Left and centre: simulation domain. Right: structure of the first internal flow diffuser.

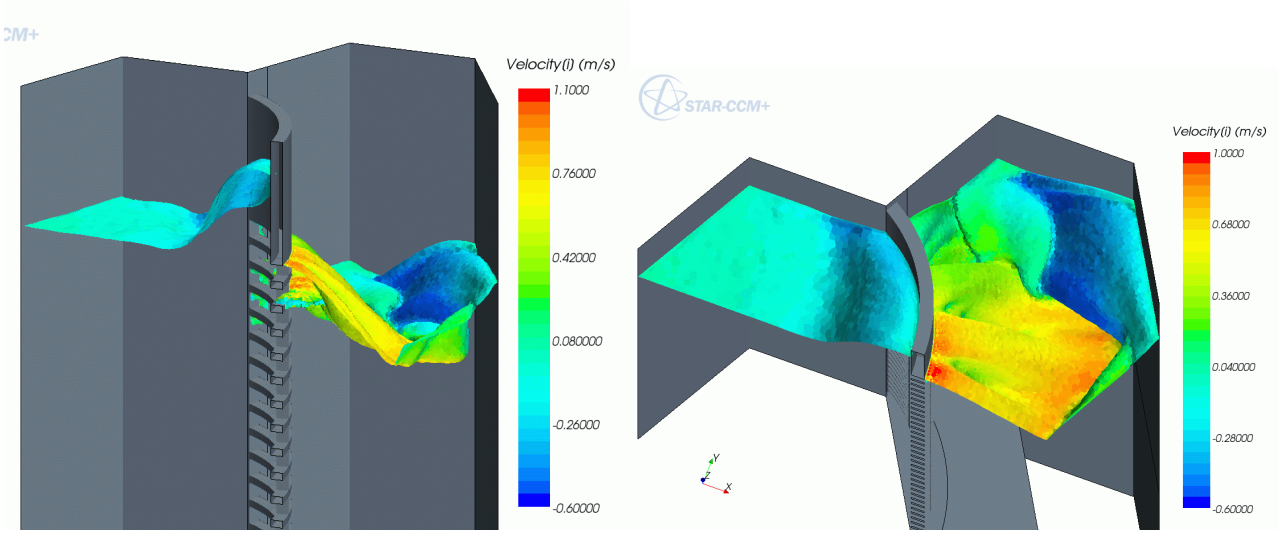

Figure 2: CRS4 target with rounded diffuser. Iso-surface (c=0.5) of volume concentration coloured by velocity magnitude.

The velocity constraint imposes to use an entire lobe as riser and so also an entire lobe as down-comer. There is therefore only one lobe surface at disposition to organize both the flow diffuser and the spallation target region.

The first trials allowed to adjust the grid differentiation to approach the desired flow configuration. In Figure 1, it can be seen that the diffuser is given a rounded shape. This was motivated by the initial desire to largely span the incoming flow. However, in this free surface context, the objective is absolutely not reached. In effect, it has been seen that it is unlikely to distribute the flow horizontally in an arc of circle from a bended diffuser because the forced flow divergence was simply resolved by unwanted light phase inclusions and an heavy phase flow separation in the expected free surface proximity. This is illustrated in Figure 2. Another point to keep in mind is

that we want to couple the flow with a beam line. We would like this beam line to span a region (to be defined) that is not too much out centred. Thus, a bended diffuser touching the centre of the target is not a so brilliant idea…

3 Planar diffuser

To avoid the formation of the finger structures shown in Figure 2, the flow diffuser would have therefore to operate only in intensity and not on the planar direction. For constructive simplicity and in absence of opposing motivation, we have restrained ourselves to a diffuser made of vertical series of small horizontal barrels with variable rectangular section and pitch. Due to erosion concern, cylindrical or at least smoothed barrels would be preferable, but require numerically a too high definition at this stage of the study.

Because of the velocity constraint and because we want to withdraw the diffuser from the centremost region, we have been forced to consider a slightly larger domain, which has been increased by one third (on an horizontal section basis). The new geometry is now built on the assembly of three hexagons of external diameter 12.2 cm. the surface mesh approximately at the free surface level at rest is shown in Figure 3.

To be consistent and compliant with a 600 Mev proton beam, which penetration depth is between 30 and 32 cms in lead or LBE, we have organized a diffuser distributing the flow on 34 cm high and kept about 5 cm of relatively stagnant fluid below the spallation region to serve as buffer.

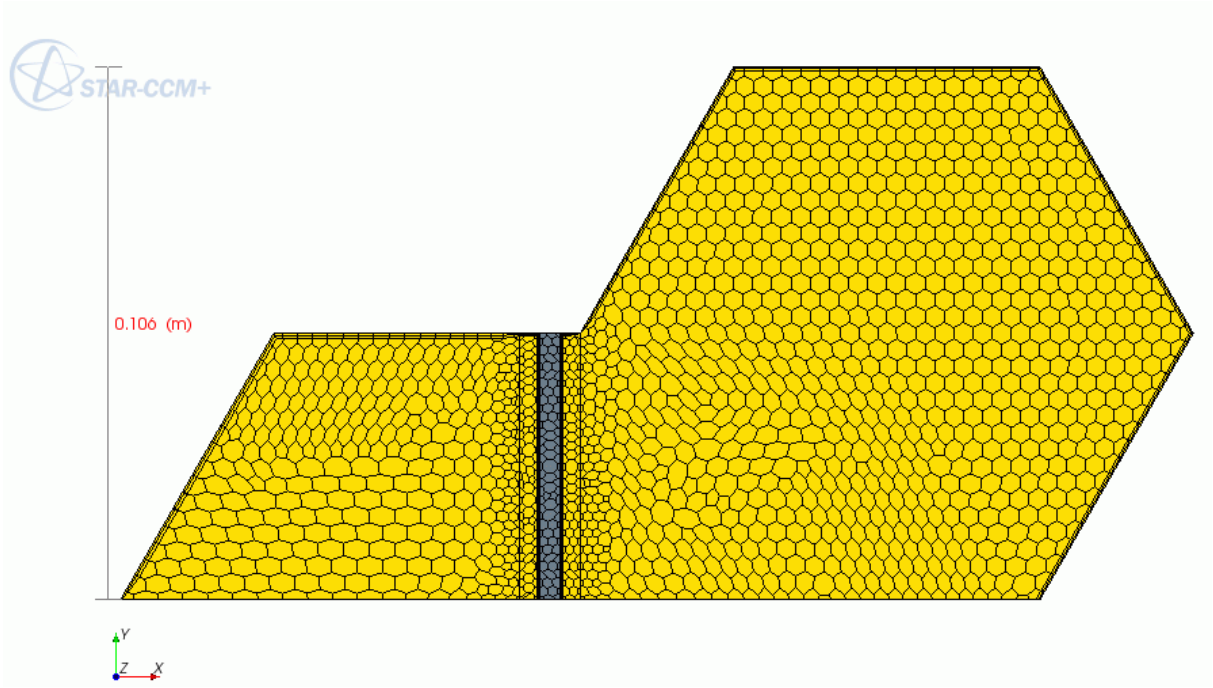

Figure 3: surface mesh of the block structure at the level of the free surface at rest

From bottom to top, the 39 cm (34 + 5) of diffuser are organized as follows:

1. from 0 to 50 mm: complete obstruction,
2. from 50 to 140 mm: 50% obstruction,
3. from 140 to 260 mm: 40 % obstruction

4. from 260 to 380 mm: 30 % obstruction.

The obstruction should be complete also at higher quotes up to a height to be better defined. In our simulation, the obstruction spans from quote 380 to 480 mm.

A test case taking into account these considerations has been run and gave good preliminary results.

The water volume flow rate has been fixed to 6.5l/s (half domain) to be compliant with the XT-ADS target requirement of 13 l/s. The pressure is fixed at zero at the top stagnation inlet, and adjusted to some value at the bottom outlet. The choice of the bottom pressure in fact essentially controls the mean free surface level. A value of 3800 Pa was found out to be satisfactory.

As shown in Figure 4, a relatively stable and sharp free surface has been obtained, both sides of the diffuser. This was enough to test several variants of the sharpening algorithm, and also to test successfully the coupling with an ultra-simplified energy release. Warned by the former free-fall simulation, we have checked the usefulness of the sharpening algorithm. The flow after 1.5s of the algorithm switched off is shown on Figure 5, showing a large smearing of the interface. On Figure 6, we show the result of a few seconds of simulation with a tentative alternative sharpening algorithm. Here the original or reference algorithm is a light phase sink equal to 50 times the product of the volume fraction: S=-50 cd, where c is the water volume fraction and d the air volume fraction. The first tested variant is a source of the form: S= 100 (d-c)cd, inspired from the Allen-Cahn equation. The result, not shown here was a smearing of the interface, slower than with no source and mainly consisting of a diffusion of water in air. The third trial has been a source made of the mean of the two precedent ones: S=-100 c^2d. The result is shown on Figure 6. Diffusion of water in air is still present. This is better seen on the right side image of the figure for which the volume fraction colour-scale is concentrated on low values. For the motivation of such source terms, refer to the theoretical document associated with these simulations. However, we have a clear indication that the simplest source term of scalar nature works best.

Turning back to the original algorithm, an oscillation of the surface and of the outlet flow rate has been observed, with a typical frequency about 1.1 Hz. The maximum temperature was particularly sensitive to this oscillation even if the flow rate oscillation was order only 4%. These aspects will be more addressed in the next simulation.

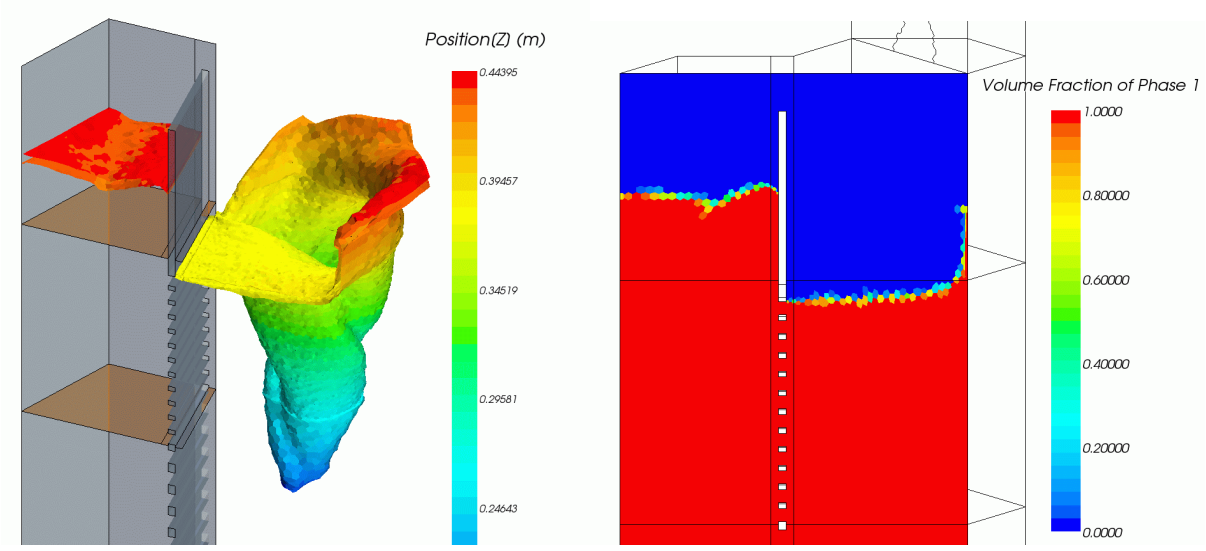

Figure 4: CRS4 target with straight diffuser. Left: two iso-surfaces of the volumetric fraction (0.1 and 0.9) coloured by height. Right: water volume fraction on the symmetry plane.

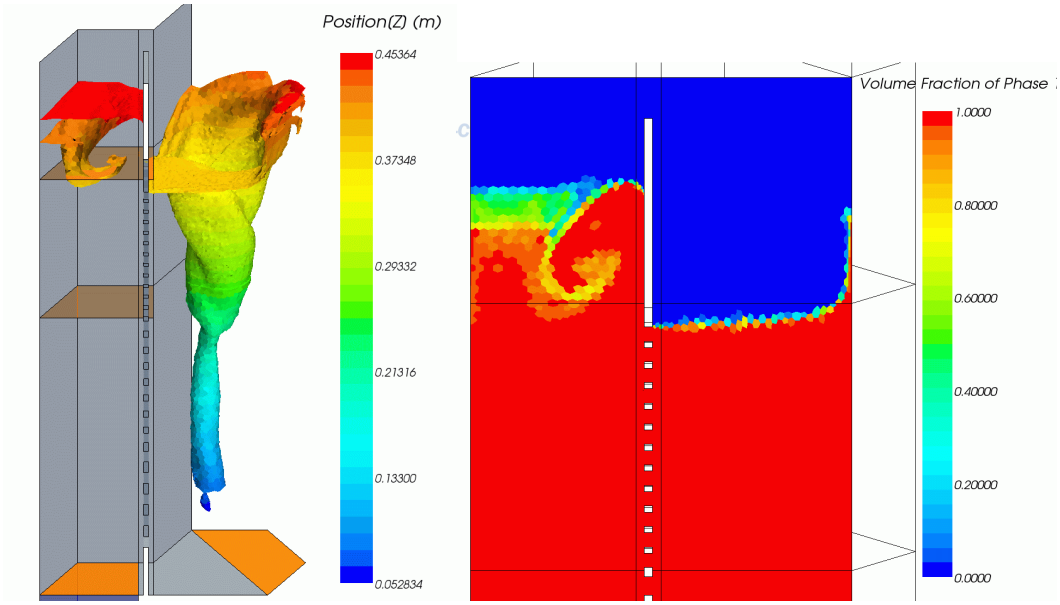

Figure 5: CRS4 target. Flow after 1.5s of simulation without sharpening algorithm. Left: volume fraction iso-surfaces 0.1 and 0.9 coloured by height. Right: related water volume fraction on the symmetry plane.

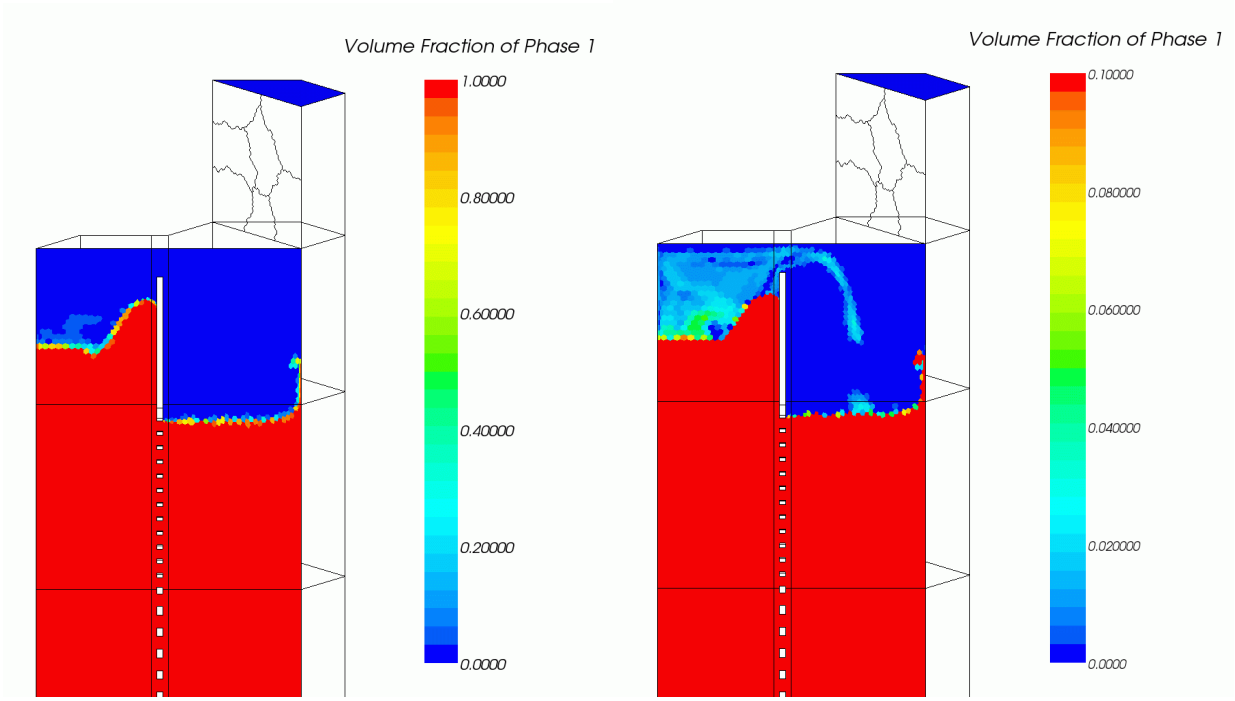

Figure 6: CRS4 target. Few seconds trial of a tentative alternative sharpening algorithm. Water volume fraction on the symmetry axis. Right: the colour scale is concentrated on the low values (between 0 and 0.1).

4 Complete loop

There was the feeling that the small flow rate oscillation (inducing a rather large maximum temperature oscillation when coupled with a simplified beam heat release) was due to excessively

forced boundary conditions. We recall that the boundary conditions were a fixed flow inlet and a pressure outlet. A second top pressure outlet allowed for variations of the light phase volume and for the stabilization of a free surface.

Closing the loop at the bottom seemed more realistic. That is what we have done. The outlet has been connected to the inlet, a bottom region has been dedicated to the resetting of the temperature and another one has been completed by a distributed momentum source simulating a generic pumping device. The complete geometry is illustrated in Figure 8. It should be noted that former trials to operate such closed Eulerian multi-phase loops systematically ended in global failure due to the slight but always increasing mixing of the two phases with an always increasing fraction of light phase entrained into the loop. Thanks to the Starccm+ VOF convection scheme aided by the sharpening/condensation feature, we can attempt a new trial with some chance of success.

A transient simulation of 48s has been performed with the following parameters:

- Mesh size: 4.0 mm, except close to the diffuser 2mm, resulting in a total of 670 k polyhedral cells with 4.3E6 interior faces.
- Time step: 0.001s, maximum inner iterations: 5.
- Top air pressure: 0.0 Pa (stagnation inlet)
- Air sink: 50 cd.

The simulation was run on 10 CPU on a PC cluster simulating about 1.5s of flow each 24 hours. The physic modelling used is resumed in Figure 7.

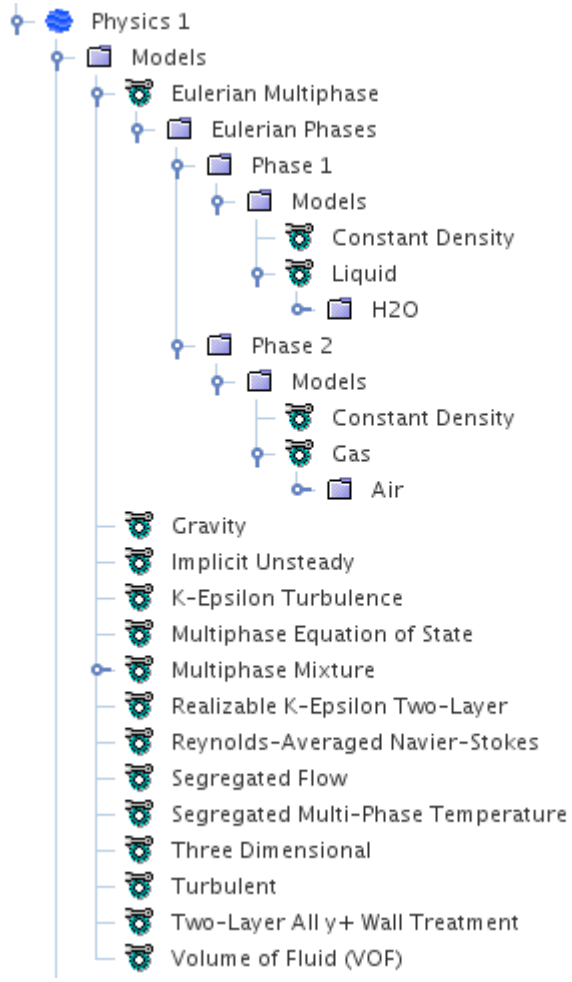

Figure 7 : physic modelling used for the starccm+ (V4.08) simulation

A closed loop means that we have to wisely choose an initial free-surface level because the overall heavy phase volume is expected to be conserved. We also have to evaluate a priori the global hydraulic resistance of the loop to dimension the pumping power intensity, so that the required flow rate is obtained. However, this can be done rather dynamically from an initial conservative guess.

At the geometric modelling stage, one tends to avoid useless volumes that will have to be meshed and will require additional computing power but will not any useful or better information. Unfortunately, usefulness of some volumes may appear too late… In our case, the plain separation in the upper part allowing the rising flow to buffer has been made too short. The available height for a stagnant flow over the riser is too short and a secondary flow path appears before we reach the desired flow rate (in this case 6.5 l/s for the half-domain). In fact, the first overflow in the simulation has not been noticed at first (it seemingly appeared during the week-end). Initial trials to get rid of the overflow by slightly lowering the pumping power were not successful. As we wanted to keep a decent flow rate, we switched strategy and started to reduce the volume of water. At the third reduction, the overflow stopped.

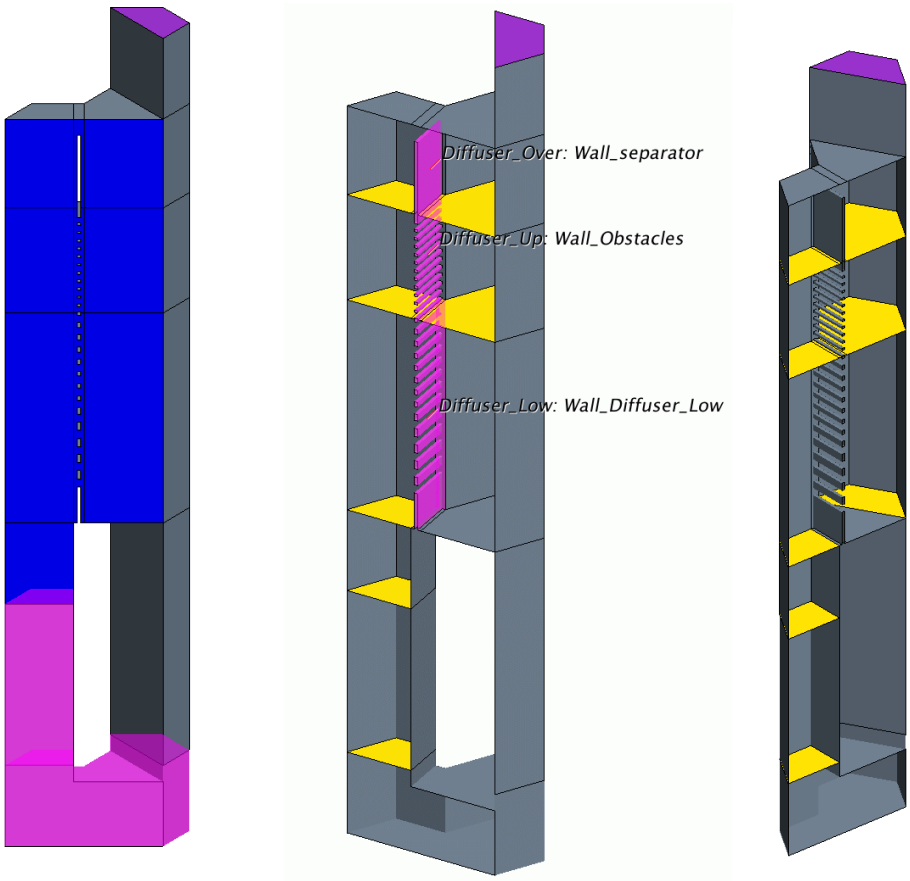

Figure 8: CRS4 target geometry. Left: highlighted are the two volumes added to close the loop. Centre: highlighted diffuser. In yellow, the volumes interfaces. In blue, symmetry plane.

The simulation has been started with a flow at rest and an initial interface coincident with the upper volumes horizontal interface. The flow is then driven by a vertical momentum source located in the volume under the former inlet. While uniform in space, the momentum source has been dynamically adjusted in time. Its intensity is reported in the Table 1, below:

Time (s)	0	5	7	9.3	11	15	17	42
f/ρ (m/s^2)	5	20	29	26	24	22	20	15

Table 1: Time evolution of the applied force intensity during the first loop transient.

The water mass flow rate has increased according to applied force and its time evolution is shown on Figure 9. In a second step, we have reduced the volume, setting a source (sink) of the water volume fraction of the form: $S = -\frac{1}{\tau * Volpump} * (VolObjective - VolActual)$, where τ is a characteristic time scale typically about 0.2 s, Volpump is the volume over which the source is applied, VolObjective and VolActual are self explanatory. The time evolution of the water volume integral is shown on Figure 10. One can see that the water volume is not fully preserve during the first 22s for which no source term is applied. There is a very slight increase of the volume seemingly due to an excessive local CFL during the overflows. The water volume has been reduced in several steps, the first one resetting the original volume and the two other one withdrawing a total of 100 cm^3, corresponding to about 7 mm in height at time 30s. From this time further, the

overflow stopped, but the mass flow oscillation did not (not even showing a decreasing tendency), as can be seen on Figure 9. The evolution of the objective water volume during the simulation is given in Table 2.

Time (s)	22	26	28	35
Objective water volume (l)	9.41	9.36	9.30	9.20

Table 2: setting and change of the objective water volume during the simulation.

The mass flow rate oscillation, about 3%, is associated with a much bigger oscillation of the free surface level over the rising flow, and by via of the volume preservation, also of the free surface level of the down-coming flow. Nevertheless, the free surface level of the spallation target region is much more stable. These aspects are better appreciated on the related animations.
With the suppression of the overflows, we could consider the flow to be regular enough to couple with a simplified heat source, mimicking some of the spallation beam features.

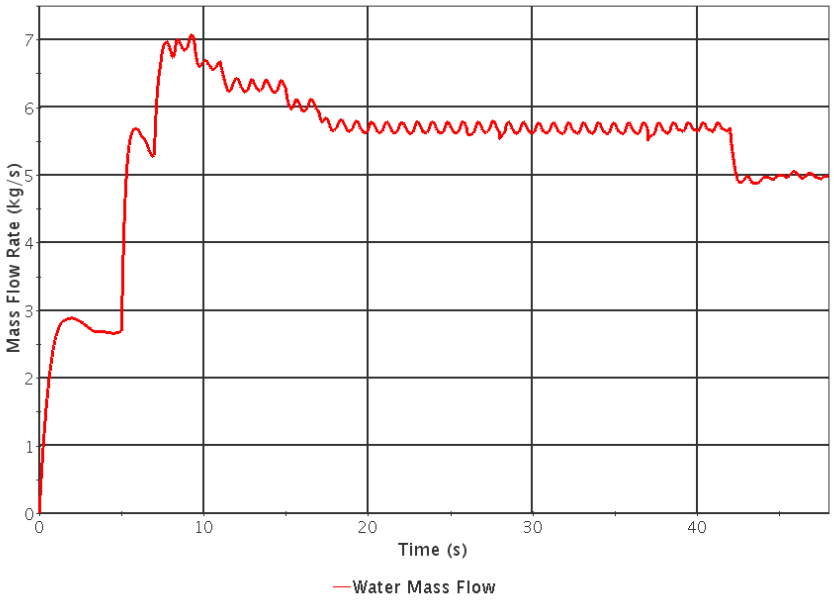

Figure 9: time evolution of the water flow rate in the loop.

When looking at the temperature fields at time 30s (without heat source) we found out that it was not uniform and there was a slight temperature increase (about 1K) in the neighbourhood of the free surface, mainly on the air side. This temperature increase is linked to the air volume fraction source term which was not accompanied by the corresponding Enthalpy source (by via of the conservative form of the equations). Setting this enthalpy source term, the temperature anomaly rapidly disappeared to be essentially absorbed at time 32s. More precisely, if S_{air} is the air volume fraction source term, then the enthalpy source term S_H is given by $S_H=\rho_{air}*Cp_{air}*T*S_{air}$. In precedence (from time 11.2s), we had tested another enthalpy sink in the bottom part of the loop, of the same shape of the water sink, so that the temperature is correctly reset to 300K in the riser. Also, another enthalpy sink was set to cope with the water withdrawing, following the same rule.

At time 32s, we have switched on a volume heat source in a parallelepiped volume in the foreseen region of the beam impact. It is proportional to the water volume fraction and otherwise constant on the volume (horizontal rectangular section [dx,dy]=[1cm, 4cm], 1kW/cm^3). It penetrates in depth up to 5 cm of the diffuser bottom for a total length about 33 cm when the free surface is horizontal and aligned with the upper diffuser opening. The lower limit is aligned with the lower diffuser opening. Its effect is to increase the flow mean temperature by slightly more than 5 degrees. The maximum temperature in time is given in Figure 11. Some illustration of the flow shape and temperature is given in Figure 12 and Figure 13 at time 35s. It must be stressed that the water density is kept constant in this simulation. So, no specific buoyancy effect can be captured. This has to be corrected in the future when we deal with LBE[5]. However, the flow is arranged in such a way that we do not foresee relevant buoyancy effects even with large temperature variations. In fact, the flow is tentatively organized so that eventual buoyancy effects would appear only for huge temperature differences, following the strategy used for the PDS-XADS channel target.
While the flow is limited in this case slightly below 6 l/s, some useful information has been obtained. First, the free surface can and does easily recover from the occasional additional jet flow from above the separator. Second, the flow is slightly pulsed in presence of this overflow (with a period about 0.9s),and further investigation demonstrate that the pulsation continue undisturbed when the overflow has been removed (by lowering the flow rate and the heavy fluid total volume).

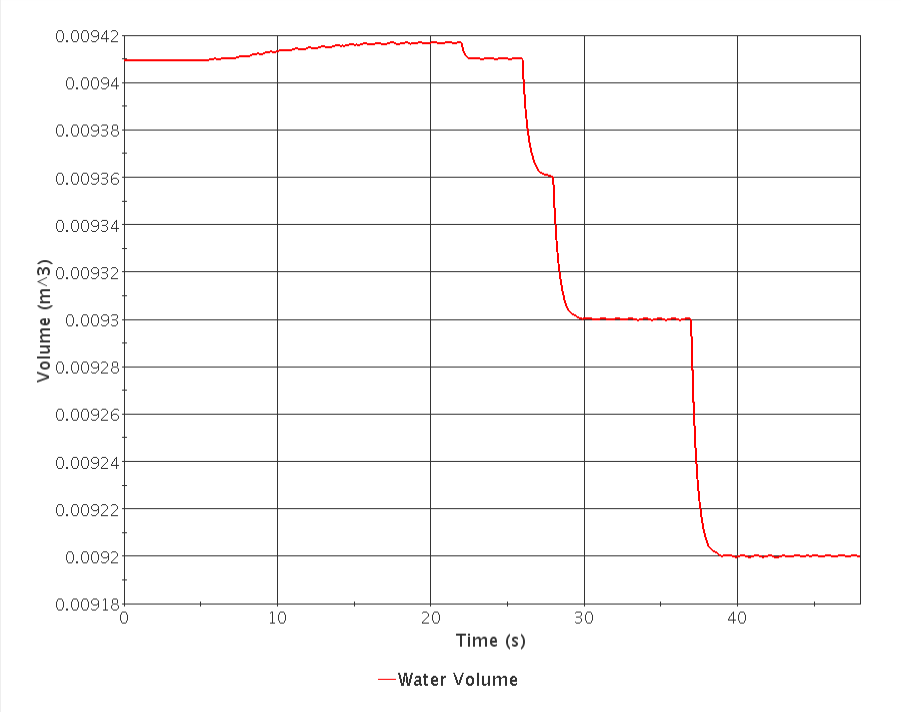

Figure 10: time evolution of the water volume integral.

[5] Lead Bismuth Eutectic

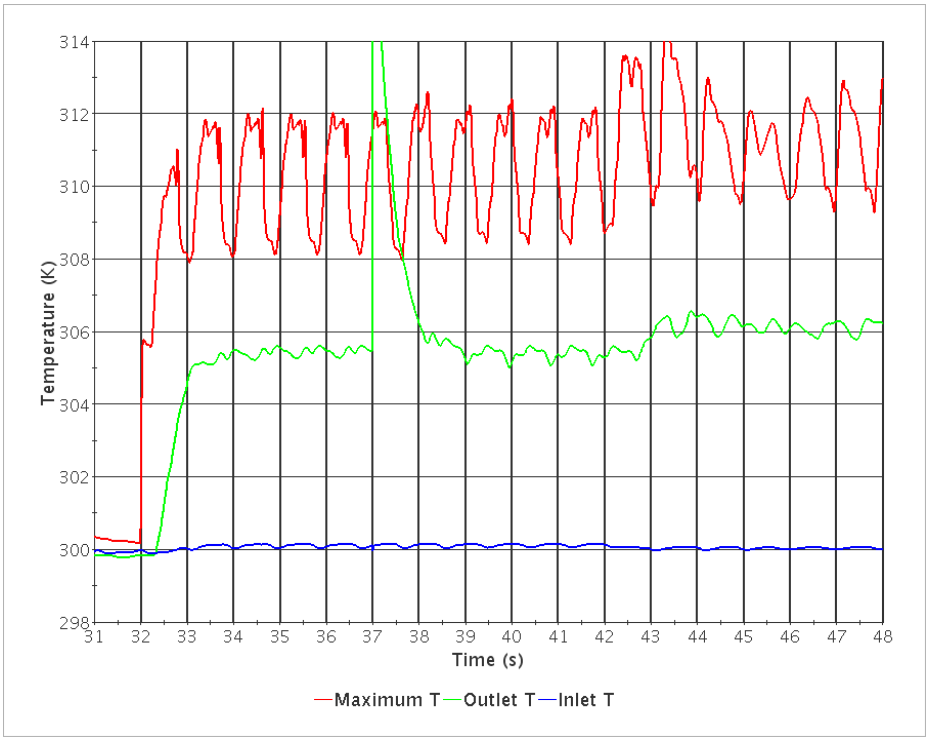

Figure 11: Time evolution of some temperatures. Red: max. T, green: mean outlet T, blue: mean inlet T.

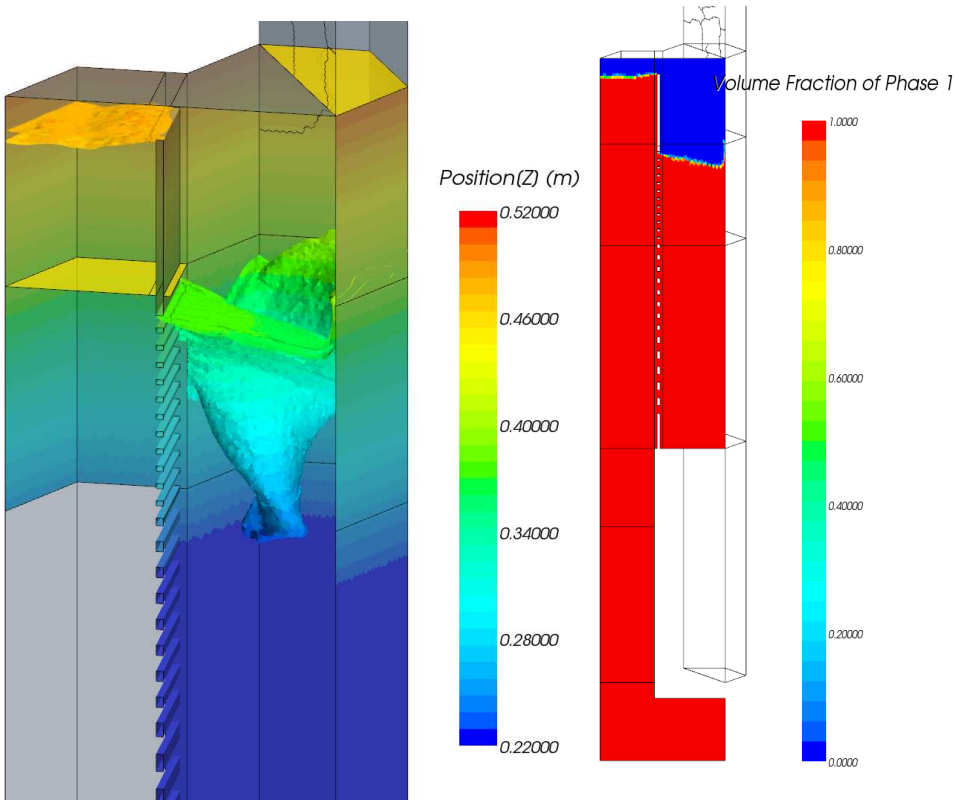

Figure 12: free surface position at time 35s. On the left, we show the two iso-surfaces 0.1 and 0.9 of the volume fraction.

So, the pulsation seems to be inherent of the geometry under these operating condition. However, while the surface level over the buffer region varies quite a lot, the flow rate in the downward sections varies only by about 3%. Furthermore, the flow is quite regular in absence of overflow close to the exit of the diffuser where the spallation beam is foreseen to impact. Only the surface slopes changes slightly. Third, the condensation is able to keep the heavy fluid integrity in the heavily stressed part of the flow where it swirls down into the two down-coming lobes. No light phase is entrained in the loop in this strongly sheared flow. Forth, the separation of the horizontal flow creates two heavy fluid rolls, one at each side, which do not rebound in the central spallation region but reverse towards the centre of the respective hexagonal lobes. The flow is cut by the re-entrance of the geometry in a similar way one can see at the prow of most ships. This feature could be eventually enhanced in upgraded versions of the design. Fifth, we have established an "existence theorem" for the feasibility of such a loop. Coupling with the beam line and operational transients are likely to be studied with meaningful results. Sixth, as shown in Figure 14, the Courant number can be kept about unit on the free surface and still this free surface is kept sharp. This allow to run the simulation at least three time faster than as recommended by CD-Adapco for this kind of flow (where the Courant number should be kept below 0.3).
The volume change operated from 35s on, was no more motivated by the elimination of the overflow but to check whether a greater stability could be attained, even at a higher flow rate, lowering some more the mean free-surface level. The result was not convincing. However, at time 42s, we have lowered again the pumping force by 25 % resulting in about 12 % less mass flow rate and a neat damping of the surface instability.

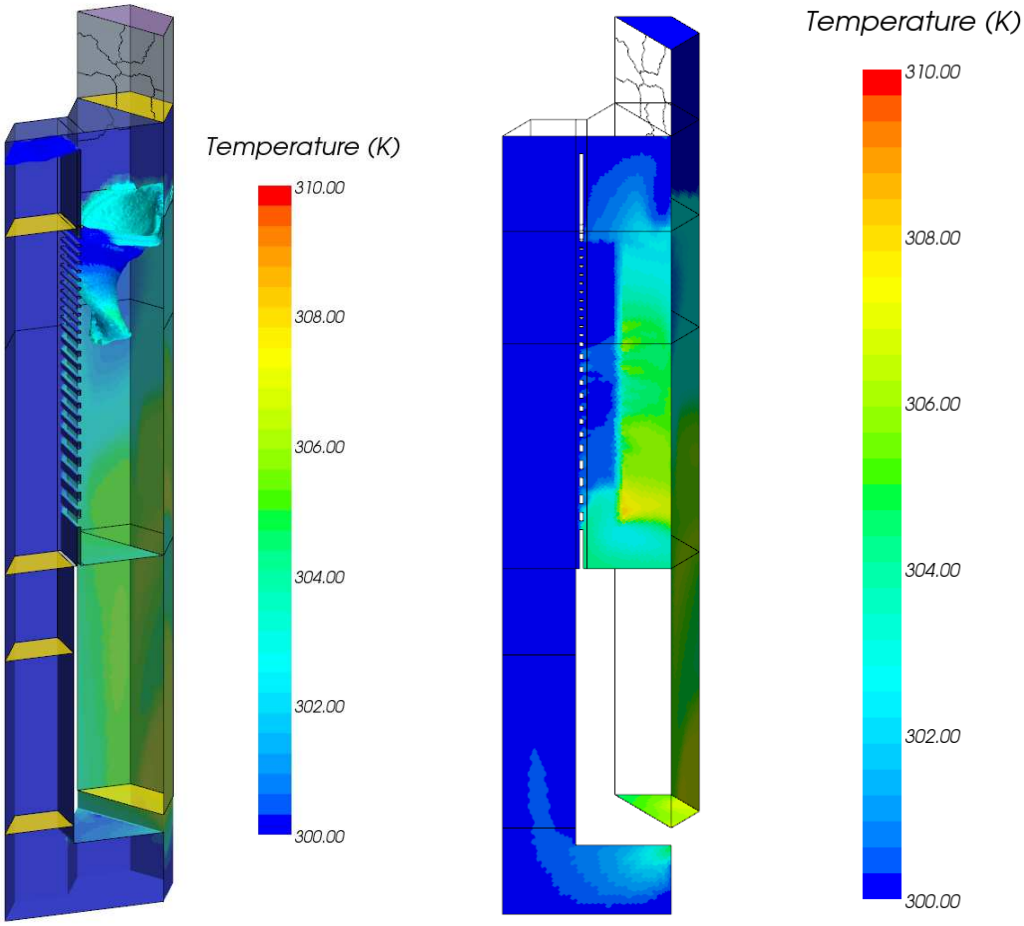

Figure 13: temperature at time 35s.

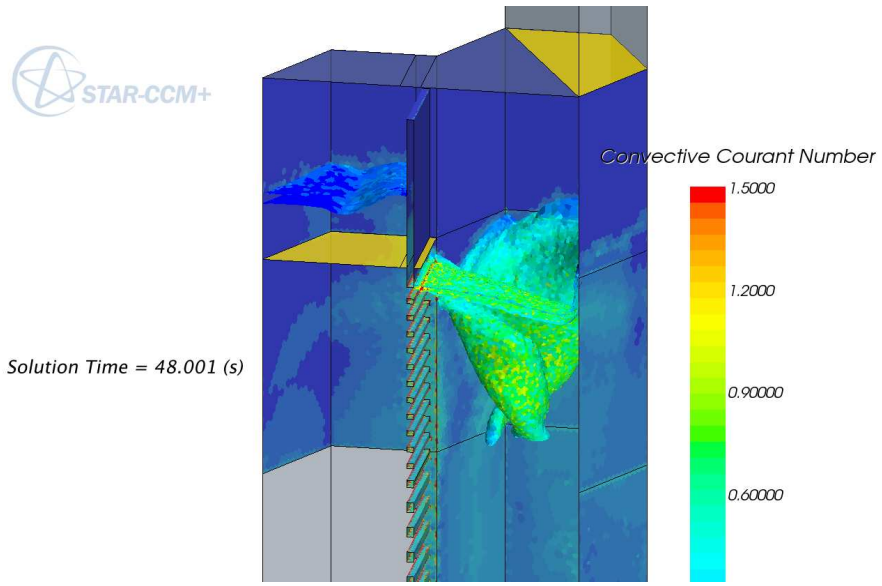

Figure 14: Convective Courant Number on the 2 iso-surfaces delimiting the free surface at time 48s

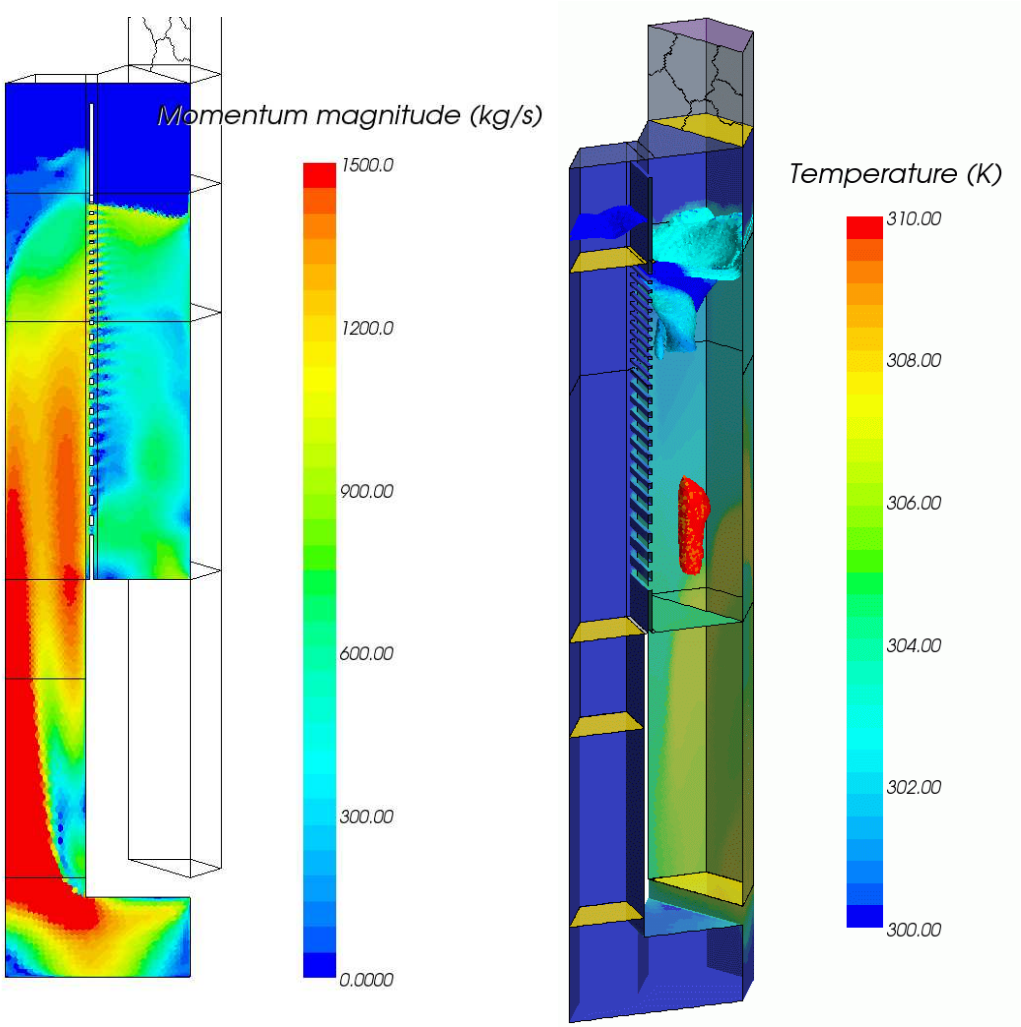

Figure 15: End of simulation, time=48s. Left: momentum magnitude on the symmetry plane. Right: the two iso-surface c=0.1 and c=0.9 coloured by temperature. In addition, the iso-surface T=310K is shown in red.

In Figure 15, we show the momentum magnitude and the temperature at the end of the simulation at 48s. It can be seen that the surface velocity is slightly above 1 m/s in the spallation region and that the maximum temperatures are usually reached in a volume located deep inside the bulk of the fluid, letting the surface much cooler.

The work reported here has been mainly performed during the first half of 2010. By, this time it has been decided that FASTEF would not use a separated spallation loop and therefore could not use a windowless target. However, the design presented could be source of inspiration for an update of an EFIT like spallation target design.

5 Conclusion

A full 3D loop with an articulated free surface and a thermal coupling has been investigated numerically with starccm+V4.06, thanks to the improvements made in the code VOF treatment and thanks to the use of a simple user based condensation/sharpening algorithm. The free-surface flow simulations presented here seem able to capture some detailed flow structures and transient behaviour which were not expected. Thanks to the simulation improved accuracy, we could visualize the rounded flow diverter defect and renounce to it. We have also been forced to consider that the free-surface was likely to present large oscillations. It is a very positive fact that these features could be now faced at this preliminary design investigation level.

In the end, what seems to be the sound basis of an alternative windowless spallation target to be used in an ADS has been presented.

6 Acknowlegment

The presented word has been financially supported partially by the Autonomous Region of Sardinia and partially by European Commission (FP7 Euratom).

7 References

[1] http://www.cd-adapco.com/.

[2] Carluec, B., jardi, X., 2003. European project PDS XADS-preliminary design studies of an experimental accelerator driven system. In: Proc. Of the Int. Workshop on P&T and ADS Development, SCK-CEN,Mol,Belgium,p. A91

[3] J.U. Knebel et al. European Research Programme for the Transmutation of HighLevel Nuclear Waste in an Accelerator Driven System (EUROTRANS), Proc. 9th Int. Exchange Meetng on Partitioning & transmutation, Nimes France, September 25-29 2006.

[4] Beaten P. et al., the Central Design Team FP7 projet, http://www-pub.iaea.org/MTCD/publications/PDF/P1433_CD/datasets/presentations/SM-ADS-09.pdf

[5] Cheng, X., THINS, http://www.ifrt.kit.edu/english/21_97.php

[6] Moreau, V., Free Fall 2D+ Simulation with StarccmV4. Calculation report 10/55. CRS4, jul 2010. http://www.crs4.it/Publications/cgi-bin/tr/repository/crs4_1534.1.doc

[7] Bianchi, F., et al, Thermo-hydraulic analysis of the windowless target system, Nucl. Eng. Des. (2008), doi: 10.1016/j.nucengdes.2007.10.026